A Low-Profile Wearable Textile Antenna Using AMC for WBAN Applications at 5.8GHz

Wahida Bouamra
Department of Physics
Faculty of Sciences of Tunis
University of Tunis El Manar
Tunis, Tunisia
bouamra-wahida@hotmail.com

Imen Sfar
Department of Physics
Faculty of Sciences of Tunis
University of Tunis El Manar
Tunis, Tunisia
imen.sfar.fst@gmail.com

Ameni Mersani
Department of Physics
Faculty of Sciences of Tunis
University of Tunis El Manar
Tunis, Tunisia
mersani.ameni@gmail.com

Lotfi Osman
Department of Physics
Faculty of Sciences of Tunis
University of Tunis El Manar
Tunis, Tunisia
lotfi.osman@supcom.tn

Jean-Marc Ribero
Department of Electronics
University Nice-Sophia Antipolis
Sophia Antipolis, France
jean-marc.ribero@univ-cotedazur.fr

Received: 25 April 2022 | Revised: 12 May 2022 | Accepted: 7 June 2022

Abstract-This paper presents a low-profile, wearable textile antenna, designed for Wireless Body Area Network (WBAN) applications operating in the 5.8GHz band for Industrial, Scientific, and Medical (ISM) applications. An Artificial Magnetic Conductor (AMC) structure was used to improve antenna performance and protect the human body from back-radiation. The antenna with the integrated AMC achieved a measured gain of 8.92dBi, an efficiency of 80%, a wide impedance bandwidth of 1.4GHz (24.1%), and SAR values of 0.00103 and 0.00034W/Kg for 10g and 1g tissues respectively. The proposed antenna was studied in a worn-on-body scenario using a multilayer numerical model of the human body. The influence of the thickness of each tissue layer of the human body was investigated. The results showed that the antenna maintained its performance, a stable gain was obtained, and the SAR values were also below the IEEE guidelines that guarantee the safety of the wearer.

Keywords-Artificial Magnetic Conductor (AMC); ISM; Specific Absorption Rate (SAR); textile antenna; WBAN applications

I. INTRODUCTION

Wearable antennas have been intensively studied, as they are widely used in WBAN applications such as health monitoring, emergency services, identification systems, enterprise, space, military rescue activities, and physical training [1]. The use of body-worn electronic devices, such as smart glasses, watches, and textiles, has grown rapidly as a result of the increasing need for wireless communication. The main interests in the implementation of these systems are well-being, health, and lifestyle [2]. As a result, Wireless Body Area Networks (WBANs) have attracted considerable attention [3]. Antenna design for WBAN systems is challenging compared to conventional systems because the human body is a dispersive medium due to its high permittivity and conductivity [3]. Many researchers studied different types of antennas to improve their performance near the human body. For example, in [3-5], monopoles with an Artificial Magnetic Conductor (AMC), a circular ring slot antenna with a SIW cavity back, and a Planar Inverted F Antenna (PIFA) were presented as wearable textile antennas that provide stable performance near the human body.

These antennas use rigid substrates, which can be uncomfortable for the human body, so different bending conditions must be considered [1]. Body antennas are best made from flexible textiles and wearable materials that naturally conform to the body surface [6]. Due to the recent rapid growth of electronic textile technology, several researchers focused on the application of flexible textile materials in antennas [7]. Since the textile antenna is bent on the human body, the effects of deformation need to be studied. Therefore, to obtain an optimal antenna design for WBAN systems, insensitivity to body effects and realization of practical wearable environments should be considered simultaneously [3]. In addition, a low-profile antenna is highly desirable to ensure comfort for the wearer. Furthermore, the Specific Absorption Ratio (SAR) must be below the normal criteria and not exceed the critical values of 1.6W/kg for 1g of tissue or 2W/kg for 10g of tissue, according to the guidelines of IEEE C95.1-1999 [8]. Furthermore, one of the challenges of using a wearable antenna is the variation in tissue thickness, especially in the fat and muscle layers. This thickness is not the same for all individuals [9]. Therefore, the effects of different thicknesses of body models on antenna performance need to be investigated. To overcome these problems, this study investigated a low-profile textile monopole antenna for WBAN applications at 5.8GHz. A 50Ω Coplanar Waveguide (CPW)

Corresponding author: Lotfi Osman

was used for the feed because it offers wider bandwidth and higher gain and needs to be metalized only on the one side. However, since the antenna must be placed near the human body, there is no ground plane to protect it from the generated back radiation. Therefore, an AMC is needed to improve antenna performance and protect the body from the effects of back radiation [6]. This study proposed a low-profile textile antenna loaded by an AMC structure with high gain, high efficiency, and good isolation while achieving low SAR level. Moreover, the influence of the thickness of each tissue layer of a human body on the proposed antenna performance was studied for the first time to ensure that the antenna adapts to all individuals while maintaining performance stability. To ensure that the proposed antenna fits different human bodies, three different body models with different tissue thicknesses and compositions were considered to study the effect of human tissue thickness on antenna performance in terms of gain and SAR.

II. ANTENNA DESIGN AND DISCUSSION

A. Antenna Geometry

The monopole antenna configuration was designed based on the design proposed in [5] and optimized for operation in the ISM 5.8GHz band. Figure 1 shows the dimensions and the fabricated prototype. The wearable antenna has a simple structure to avoid manufacturing complexities with overall dimensions of 14×22×0.58mm. The antenna was printed on a flexible polyester textile substrate with a dielectric constant ε_r=2.22, loss tangent tanδ=0.004, and a thin thickness of 0.5mm. The conductive layer was made of a 0.08mm thick pure electro-textile copper taffeta from less EMF [5, 10] with a conductivity of 2.5×10^5S/m. It was smooth, soft, lightweight, pliable, and easy to cut and sew. A 50Ω CPW was chosen to feed the antenna. Design and simulations were carried out using CST Microwave Studio [11, 12]. The antenna was fabricated with the optimized dimensions listed in Table I.

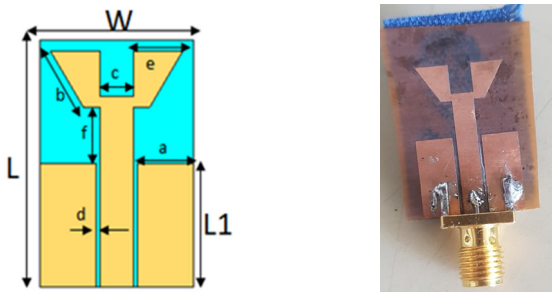

(a) (b)

Fig. 1. Geometry of the proposed antenna: (a) front view, (b) photograph of the manufactured prototype.

TABLE I. OPTIMIZED DIMENSIONS OF THE PROPOSED ANTENNA

Parameter	W	L	L1	a	b	c	d	e	f
Value	32	22	11	5.1	5	3	0.2	4.5	5

B. Parametric Study

Figure 2(a) shows the evolution steps of the proposed antenna design. The design process was divided into three stages (Ant 0, Ant 1, and Ant 2) to achieve the final design. The method used was to cut out both sides of the patch and insert a slot to achieve the desired resonant frequency by controlling the reflection coefficient parameters. Figure 2(b) shows the reflection coefficients *S11* of the three stages. The first antenna (Ant 0) is a simple CPW antenna structure, which had a good impedance matching characteristic with a wide impedance bandwidth. The two sides of the patch were truncated in Ant 1, resulting in better impedance matching, but caused a shift in the resonant frequency from 5.94GHz to 6.25GHz. In the final step, a slot was added to the patch to achieve the desired frequency. This variation also resulted in a good impedance match (*S11*= -58dB) and a wide bandwidth of 2.18GHz (4.69-6.87GHz).

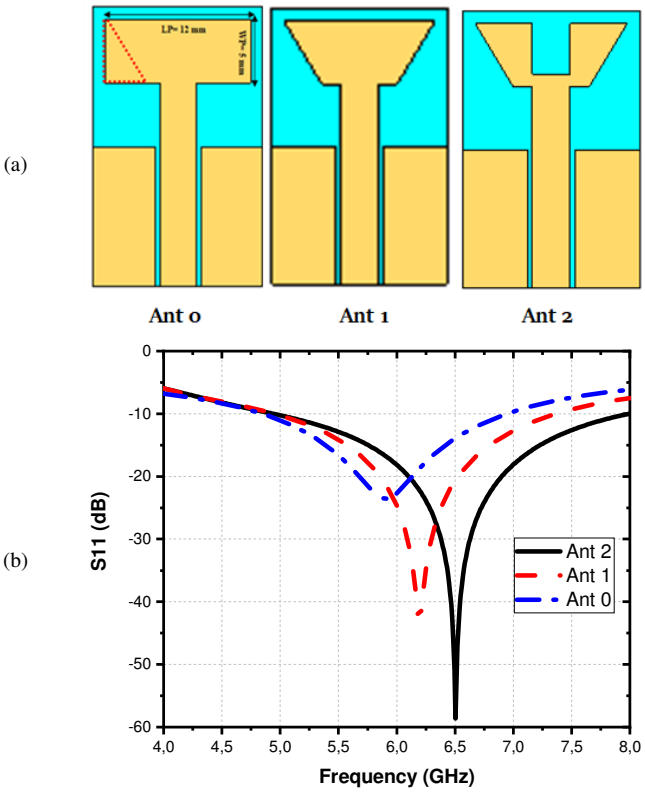

Fig. 2. (a) Evolution steps of the design of the proposed antenna, (b) corresponding *S11* reflection coefficients.

The effect of parameter *X* and the width of slot *C* on the antenna's impedance matching was examined. The antenna performance was examined for a variable length of *X* from 4 to 1.5mm, as shown in Figure 3(a). As the length of *X* decreased, better impedance matching was achieved, and the center frequency of the reflection coefficient shifted to higher frequencies. Figure 3(b) shows that varying *C* from 2 to 6mm resulted in a significant increase in impedance matching with an improvement in impedance bandwidth of about 600MHz.

Figure 4 shows the simulated and measured reflection coefficients of the antenna with optimal dimensions. Good agreement was found in terms of bandwidth between simulation and measurement at the resonant frequency. The simulated -10dB impedance bandwidth was 2.18GHz (4.692-

6.872GHz), while the measured bandwidth was 2.27GHz (4.55-6.82GHz), which largely covers the desired band. However, the measured *S11* was 26 dB lower than the simulated value due to imperfections during the manufacturing process.

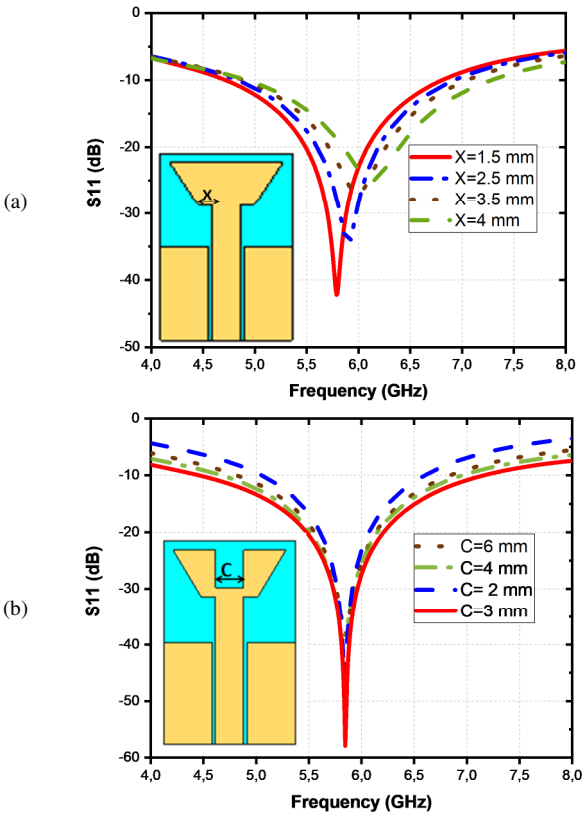

Fig. 3. Influence of parameters on the S11 performance of the proposed antenna: (a) effect of truncation width *X*, (b) slot width *C*.

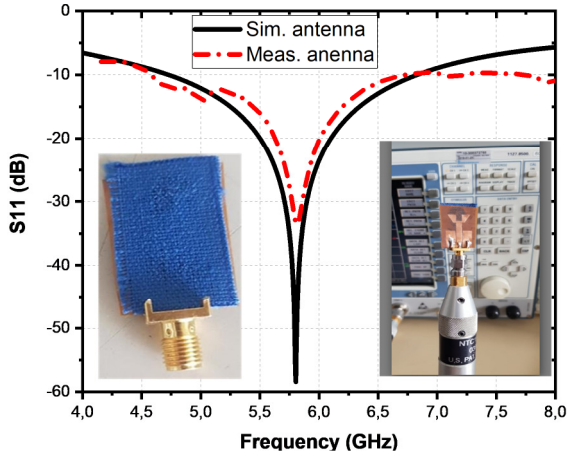

Fig. 4. Simulated and measured *S11* of the antenna.

III. AMC-BACKED ANTENNA DESIGN AND RESULTS

A. AMC Unit Cell Design

The AMC structure is a good candidate for a reflective plane of the radiated wave in wearable antenna applications, as it reduces the radiation absorbed by the human body and improves performance [1, 4]. Since the CPW antenna does not have a reflective plane and emits back-radiation, it should be isolated from the human body. Several studies used various basic classical geometric shapes (square, triangle, circle, and cross) to form a wide and two-band AMC surface [5, 8, 13-15]. This study focused on a hexagonal structure on textile because of its advantages in terms of size and bandwidth [13]. Figure 5 shows the extended dimensions of the AMC unit cell. The unit cell structure was developed on a felt substrate with a relative dielectric constant (ε_r) of 1.22, a loss tangent (tanδ) of 0.016, and a thickness of 2mm. The conductive material was copper taffeta. During the design of the AMC structure and the simulation phase, the AMC network was extended by one row and one column at a time until optimal performance in terms of gain and Forward-to-Backward Ratio (FBR) was achieved. A good impedance match was achieved within 5.8GHz. The dimensions of the different structures were adjusted to achieve a 0° phase around 5.8GHz. The frequency bands were determined by variations of ±90° around the 0° phase values, as shown in Figure 5.

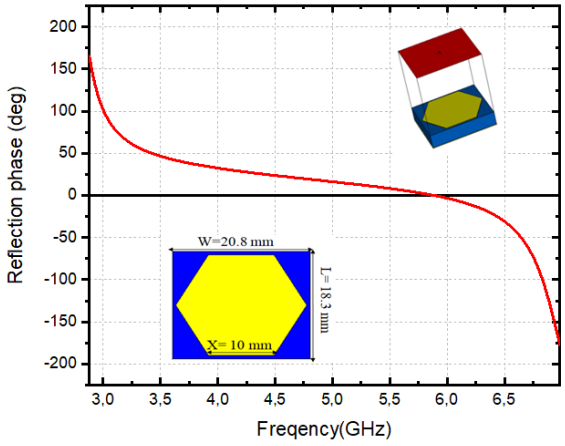

Fig. 5. Structure and simulated reflection coefficient phase of the AMC unit cell.

B. Integration of the Textile Antenna and AMC Surface

Figure 6(c) shows the manufactured prototype AMC antenna. The monopole antenna was built on an AMC layer with 2×2 units αvδ total dimensions of 34.8×39mm. A gap of 1mm thickness separated the antenna from the AMC to minimize mismatch and electrical contact and avoid short circuits [8]. A foam-like Rohacell substrate was placed in this space without changing the properties of the AMC antenna structure. The expected impedance matching and radiation characteristics of the AMC antenna at 5.8GHz WBAN applications were achieved by optimizing the geometric dimensions of the monopole antenna and the AMC unit cell.

C. Measurement Results and Discussion

Figure 7 shows the measured reflection coefficient *S11* of the AMC antenna and the simulated results. It is noted that the simulated bandwidth is larger from 5.70 to 7.10GHz (24.1%) than the measured one, which ranges from 5.71 to 6.75GHz

(17.9%). This small deviation may be due to uncertainty in the properties of the textile support and mechanical inaccuracies. Note that all results can cover the ISM band of 5.8GHz, which ensures that the proposed antenna can meet the requirements for 5.8GHz WBAN applications.

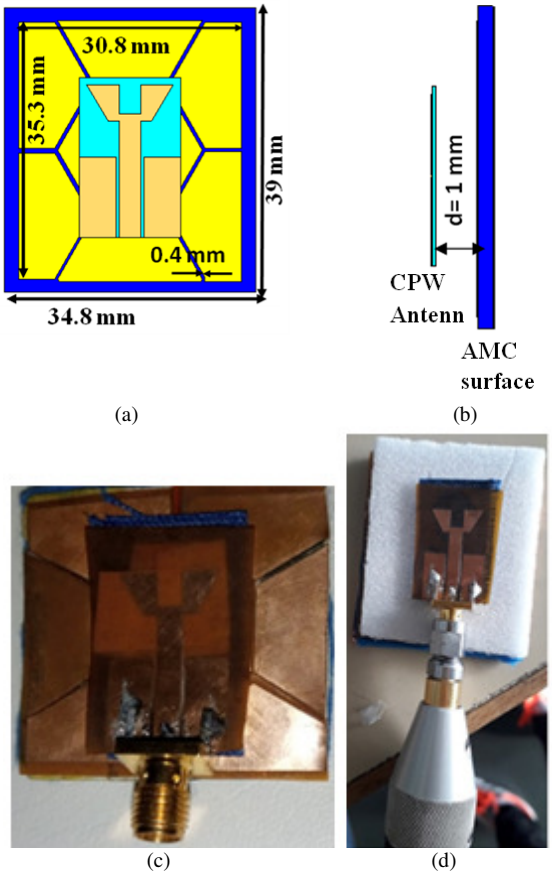

Fig. 6. AMC antenna: (a) configuration of antenna on AMC, (b) bottom view, (c) manufactured prototype, (d) measuring reflection coefficient S11.

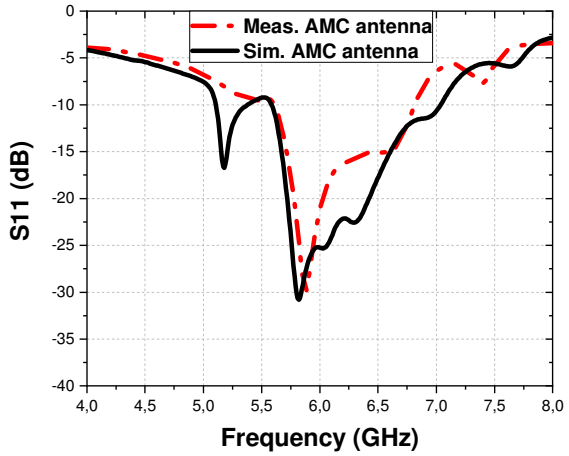

Fig. 7. Simulated and measured reflection coefficient of the AMC antenna.

Figure 8 shows the radiation pattern measurements performed in the anechoic chamber of Orange Labs in the *E* and *H* planes at 5.8GHz of the antenna with and without AMC. The results show that the AMC antenna has stronger forward radiation, while the backward radiation was reduced by 20dB by the AMC reflector plane. Thus, it was possible to reduce the backward scattering wave toward the human body.

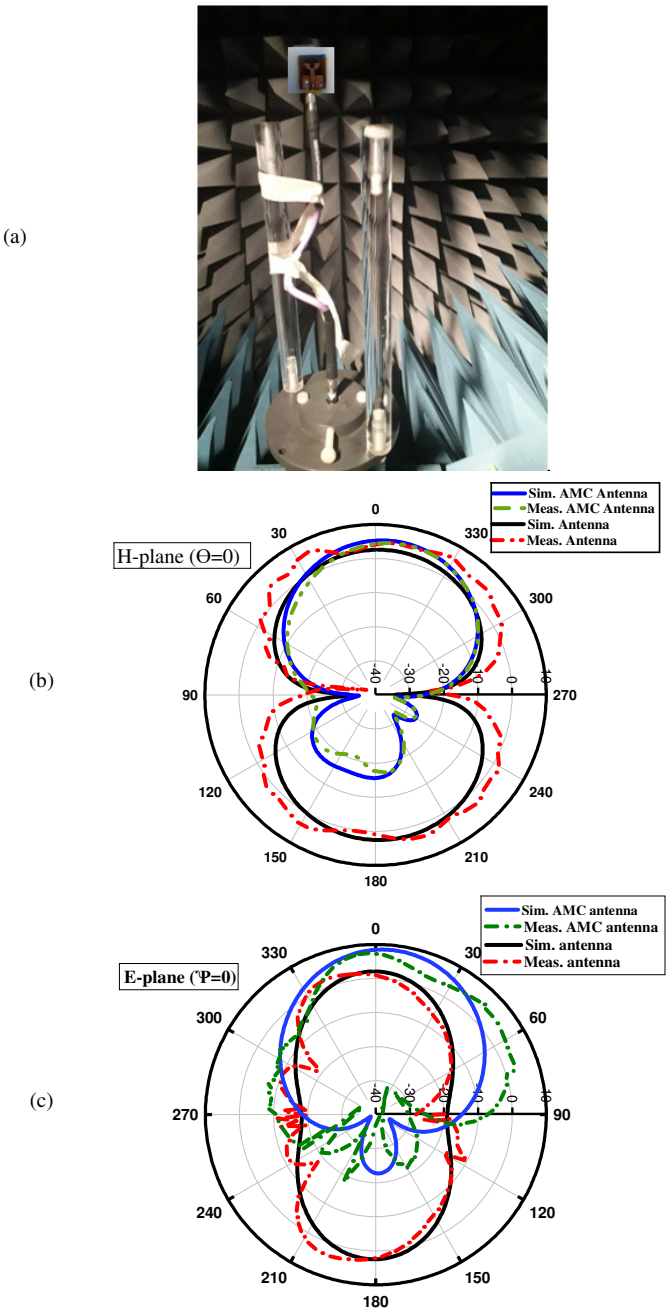

Fig. 8. Measured radiation patterns of the antenna with and without AMC at 5.8GHz: (a) Measured performances of the AMC antenna in the anechoic chamber, (b) E-plane, and (c) H-plane.

Figure 9 shows the measured gain and efficiency of the antenna with and without AMC. The measured gains of the antenna with and without AMC are 8.92 and 2.5dBi respectively. Due to the hexagonal shape of the AMC surface, the achieved gain is higher than the existing antennas'. The

maximum measured efficiency of the antenna without AMC was 60%, while the measured efficiency of the antenna with AMC was almost 79.96% at 5.8GHz. These values show that the proposed AMC textile antenna is very efficient.

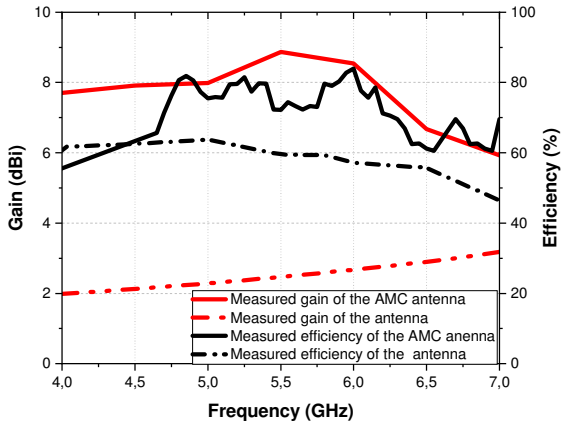

Fig. 9. Simulated and measured gain and efficiency of the textile antenna with and without AMC.

IV. ANTENNA ON THE HUMAN BODY

A. Antenna Performance in Bending Configuration

In mobile systems, a wearable antenna is often bent as a result of the movement of the human body. To study the performance of the AMC textile antenna in a dynamic body environment and under deformation, it was bent over a cylinder with a radius *R* of 60mm, representing the middle arm, in two planes (*E* and *H*). Figure 10 shows the simulated *S11* of the proposed AMC antenna in flat and bent conditions in the *E*- and *H*-plane. This figure shows that the bandwidth remained stable in both bending conditions and covered the 5.8GHz band.

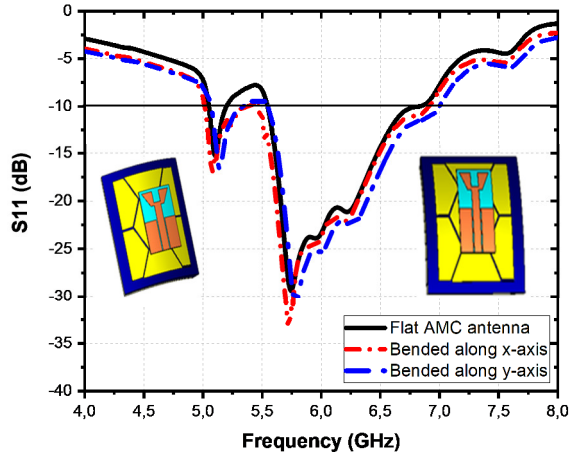

Fig. 10. Simulated reflection coefficient of the AMC-antenna in bending conditions in both *E* and *H* planes.

It is necessary to validate the performance and study the effects of human body loading on the proposed antenna. To reduce the simulation time, a 3D numerical model was studied. This model consisted of three layers representing skin, fat, and muscle tissue from the outside to the inside. The properties of the dispersive human tissue layers were taken from [16-18] and are shown in Figure 11.

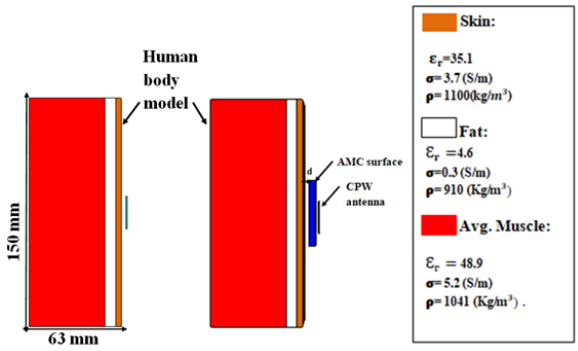

Fig. 11. Modeling the 5.8GHz antenna with and without AMC on the human body model.

Figure 12 shows that after removing the AMC surface the resonant frequency shifted toward the lower band due to the high dielectric properties of human tissue [19]. This removal also affected the attenuation of the reflection coefficient and the detuning of the resonant frequency. On the other hand, the required operating bands of the AMC antenna were achieved due to the high isolation provided by the AMC. It can be noted that the reduction of the distance *d* between the antenna and the human body model leads to a mismatch of the reflection coefficient *S11*. Therefore, protection from electromagnetic radiation was provided by a distance of 4mm between the AMC antenna and the tissues of the multilayer models.

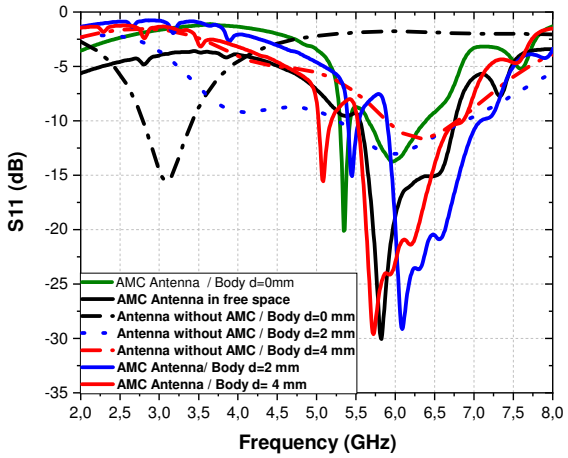

Fig. 12. Reflection coefficient of the proposed antenna with and without AMC, according to distance from the human body model (0-4mm).

The antenna was placed directly on the skin of the arm, as shown in Figure 13, and the reflection coefficient antenna was also plotted when placed on the body. The two results are close to each other. The differences compared to free space are negligible and cover the frequency band.

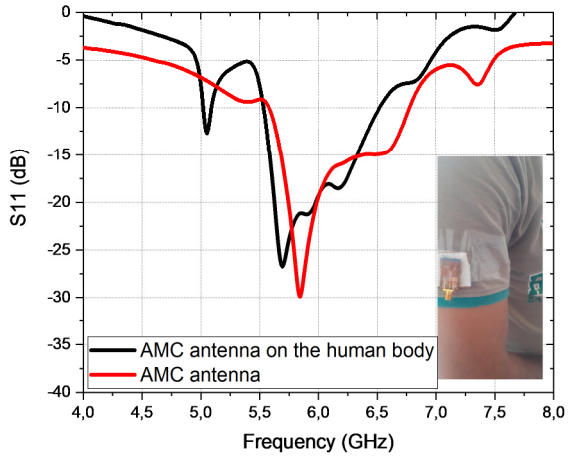

Fig. 13. Measured reflection coefficient.

B. SAR Validation

SAR was used to examine the health risks posed by portable antennas on the human body. According to the guidelines of the IEEE standards C95.1-1999 [20] and C95.1-2005 [21], the RF energy absorbed by human tissue should not exceed the critical values of 1.6W/kg for 1g of tissue or 2W/kg for 10g of tissue. SAR is given by a temporal derivative of the incremental energy (dW) scattered in an incremental mass (dm) contained in a volumetric element (dV) with a data density (ρ) [22], calculated by:

$$SAR = \frac{d}{dt}\left(\frac{dW}{dm}\right) = \frac{d}{dt}\left(\frac{dW}{\rho dV}\right) \text{(W/Kg)} \quad (1)$$

$$SAR\ (W/Kg) = \frac{\sigma E^2}{\rho} \quad (2)$$

where σ represents the conductivity in (S/m), ρ designates the mass density in (Kg/m^3), and E represents the electric field in (V/m). SAR is related to the internal E-field by:

$$E = \left(\frac{\sigma}{\rho} SAR\right)^{1/2} \quad (3)$$

$$J = (\sigma \rho SAR)^{1/2} \quad (4)$$

A numerical assessment of SAR can be performed in case of a lack of equipment and the high cost of experimentally determined SAR values. This work examined various numerical SAR studies based on mass-averaged methods using the IEEE C95.1 standard included in the CST MWS software. The simulated 1g and 10g average SAR at 5.8GHz for the antenna with and without AMC on humans are shown in Table II. The obtained results show that the presence of the AMC surface reduces SAR and provides better protection to the human body. In both cases, the SAR values of the AMC antenna were lower than the SAR limits, which guarantees its safe use.

TABLE II. SIMULATED SAR OF ANTENNA WITH AND WITHOUT AMC

***SAR* (W/Kg)**	**1g tissue**	**10g tissue**
Antenna without AMC	0.038	0.14
Antenna with AMC	0.000103	0.000349

C. Effects of Tissue Thickness on the AMC Antenna

The thickness of the tissue layers, especially fat and muscle, varies from person to person. Therefore, keeping the skin thickness constant at the average standard measurement of 3.6mm [5], different combinations of thickness values for fat and muscle layers can be studied for imaging multiple individuals [9]. Table III shows the parameters of three proposed models with different combinations, to examine how SAR can be affected by the different thicknesses of human tissue layers. The thickness of the fat and muscle layers changed, while the thickness of the skin layer remained unchanged. In the first case, the thickness of the fat layer ranged from 7 to 27mm, whereas in the second, the thickness of the muscle layer varied from 23 to 63mm, while the third had simultaneous changes in the fat and muscle layers. Furthermore, many thickness combinations of the fat and muscle layers with a total thickness of 60mm were considered.

TABLE III. THREE EXAMPLES OF DIFFERENT HUMAN MUSCLE AND FAT LAYERS THICKNESS

Case	**Tissues**	**Thickness (mm)**				
		a	**b**	**c**	**d**	**e**
1	Skin, S	3.6	3.6	3.6	3.6	3.6
	Fat, F	7	12	17	22	27
	Muscle, M	50	50	50	50	50
2	Skin, S	3.6	3.6	3.6	3.6	3.6
	Fat, F	7	7	7	7	7
	Muscle, M	23	33	43	53	63
3	Skin, S	3.6	3.6	3.6	3.6	3.6
	Fat, F	7	12	17	22	27
	Muscle, M	53	48	43	38	33

Table IV shows the 1g and 10g SAR, as well as the gain distribution for the AMC antenna in different types of the human body at 5.8GHz. In the first case, where the fat layer increased while the size of the muscle and skin layers remained constant, a decrease in both SAR values was observed. In model 2, where the muscle layer increased, the SAR values were almost stable. In case 3, where the thickness of the fat and muscle layers was changed simultaneously, a small increase in SAR values was observed, but it is noteworthy that all these values were below the normal SAR criteria. In summary, the gain and SAR values remained almost unchanged in all cases when the thickness of the different layers was varied, ensuring that the proposed AMC antenna is a strong candidate for WBAN applications for different wearers.

TABLE IV. 1G AND 10G SAR FOR THE AMC ANTENNA IN VARIOUS PROTOTYPES OF THE HUMAN BODY AT 5.8GHZ

Case		**a**	**b**	**c**	**d**	**e**
1	***SAR* (W/Kg)/ 1g**	0.46	0.45	0.43	0.42	0.42
	***SAR* (W/Kg) /10 g**	0.18	0.17	0.17	0.16	0.16
	Gain (dBi)	8.29	8.32	8.32	8.38	8.26
2	***SAR* (W/Kg) /1g**	0.25	0.25	0.26	0.25	0.25
	***SAR* (W/Kg) /10 g**	0.09	0.10	0.09	0.10	0.10
	Gain (dBi)	8.24	8.23	8.24	8.24	8.23
3	***SAR* (W/Kg) /1g**	0.41	0.47	0.42	0.43	0.45
	***SAR* (W/Kg) /10g**	0.16	0.181	0.164	0.169	0.17
	Gain (dBi)	8.29	8.29	8.29	8.29	8.29

TABLE V. COMPARISON OF THE PROPOSED AMC ANTENNA TO OTHER STUDIES

Ref	Freq. (GHz)	Dim (mm) /Reflector type	BW (GHz)		Gain (dBi)		*SAR* (W/kg)		Radiation efficiency (%)
			FS	HBM	FS	HBM	1g	10g	
[3]	5.8	75×42×1 / Ground plane	5.65-5.88 (3.96%)	5.62-5.97 (6.10)	-	3.12	-	-	37.7
[5]	5.8	102×68×3.6 / AMC	4.30-5.90 (27.5%)	-	6.12	-	0.61	1.49	-
[23]	5.5	46x36x2 / Ground plane	5.05-6.04 (18%)	5.13-5.93 (14.54)	5.9	5	0.9307	0.4016	74.1
[24]	5.5	42x28x4 / Meta surface	4.96-5.90 (17%)	4.96-5.90 (17%)	6.7	-	0.3699	0.2170	77
This work	5.8	34.8×39×4.58/ AMC	5.70-7.10 (24.1%)	5.8-7.23 (24.65%)	8.92	8.29	0.00103	0.000349	79.96

D. Comparative Study

Table V shows the performance comparison of the proposed wearable textile antenna with WBAN antennas proposed in other studies. It can be noted that the proposed antenna not only has the advantage of conformability and flexibility when worn on the human body due to the textile substrate but also has several advantages in terms of size and performance, such as high gain, low SAR, bandwidth that is not affected when worn, and is still sufficient for the application.

V. CONCLUSION

This study proposed a textile antenna for wearable applications operating in the 5.8GHz ISM band. A flexible textile AMC structure was used to protect the human body from back radiation and improve performance in terms of gain and efficiency. The antenna design had reduced dimensions of 34.8×39mm and 4.58mm thickness. The wearable AMC antenna was examined in free space and on the human body. To ensure that the proposed antenna fits different human bodies, a study on the effects of the thickness of each tissue layer of a human body model on the antenna was conducted, which showed good and stable performance. These characteristics make the proposed wearable antenna a good candidate for WBAN applications.

ACKNOWLEDGMENT

This study was conducted in collaboration with the Lab of Electronics, Antennas, and Telecommunications (LEAT) of the University of Sophia Antipolis, Nice, France, and the measurements were performed in the anechoic chamber of Orange Labs.

REFERENCES

[1] A. Y. I. Ashyap *et al.*, "An Overview of Electromagnetic Band-Gap Integrated Wearable Antennas," *IEEE Access*, vol. 8, pp. 7641–7658, 2020, https://doi.org/10.1109/ACCESS.2020.2963997.

[2] S. Alotaibi and A. A. Alotaibi, "Design of a Planar Tri-Band Notch UWB Antenna for X-Band, WLAN, and WiMAX," *Engineering, Technology & Applied Science Research*, vol. 10, no. 6, pp. 6557–6562, Dec. 2020, https://doi.org/10.48084/etasr.3904.

[3] Y. Hong, J. Tak, and J. Choi, "An All-Textile SIW Cavity-Backed Circular Ring-Slot Antenna for WBAN Applications," *IEEE Antennas and Wireless Propagation Letters*, vol. 15, pp. 1995–1999, 2016, https://doi.org/10.1109/LAWP.2016.2549578.

[4] A. Bousselmi, A. Gharsallah, and T. P. Vuong, "A Novel High-Gain Quad-Band Antenna with AMC Metasurface for Satellite Positioning Systems," *Engineering, Technology & Applied Science Research*, vol. 9, no. 5, pp. 4581–4585, Oct. 2019, https://doi.org/10.48084/etasr.2933.

[5] A. Alemaryeen and S. Noghanian, "On-Body Low-Profile Textile Antenna With Artificial Magnetic Conductor," *IEEE Transactions on Antennas and Propagation*, vol. 67, no. 6, pp. 3649–3656, Jun. 2019, https://doi.org/10.1109/TAP.2019.2902632.

[6] S. Mallavarapu and A. Lokam, "Circuit Modeling and Analysis of Wearable Antennas on the Effect of Bending for Various Feeds," *Engineering, Technology & Applied Science Research*, vol. 12, no. 1, pp. 8180–8187, Feb. 2022, https://doi.org/10.48084/etasr.4699.

[7] T. Kaufmann and C. Fumeaux, "Wearable Textile Half-Mode Substrate-Integrated Cavity Antenna Using Embroidered Vias," *IEEE Antennas and Wireless Propagation Letters*, vol. 12, pp. 805–808, 2013, https://doi.org/10.1109/LAWP.2013.2270939.

[8] A. Y. I. Ashyap *et al.*, "Compact and Low-Profile Textile EBG-Based Antenna for Wearable Medical Applications," *IEEE Antennas and Wireless Propagation Letters*, vol. 16, pp. 2550–2553, 2017, https://doi.org/10.1109/LAWP.2017.2732355.

[9] J. Mao, H. Yang, Y. Lian, and B. Zhao, "A Five-Tissue-Layer Human Body Communication Circuit Model Tunable to Individual Characteristics," *IEEE Transactions on Biomedical Circuits and Systems*, vol. 12, no. 2, pp. 303–312, Apr. 2018, https://doi.org/10.1109/TBCAS.2018.2798410.

[10] "Electromagnetic Field Shielding Fabrics - High Tech and Industrial," *Less EMF*. https://lessemf.com/.

[11] R. Dewan, M. K. A. Rahim, M. R. Hamid, and M. F. M. Yusoff, "Analysis of Wideband Antenna Performance over Dual Band Artificial Magnetic Conductor (AMC) Ground Plane," *Applied Mechanics and Materials*, vol. 735, pp. 273–277, 2015, https://doi.org/10.4028/www.scientific.net/AMM.735.273.

[12] *CST Microwave Studio*. Framingham, MA, USA: Computer Simulation Technology, 2016.

[13] M. Mantash, A. C. Tarot, S. Collardey, and K. Mahdjoubi, "Design methodology for wearable antenna on artificial magnetic conductor using stretch conductive fabric," *Electronics Letters*, vol. 52, no. 2, pp. 95–96, 2016, https://doi.org/10.1049/el.2015.3135.

[14] M. El Atrash, M. A. Abdalla, and H. M. Elhennawy, "A Compact Highly Efficient Π-Section CRLH Antenna Loaded With Textile AMC for Wireless Body Area Network Applications," *IEEE Transactions on Antennas and Propagation*, vol. 69, no. 2, pp. 648–657, Oct. 2021, https://doi.org/10.1109/TAP.2020.3010622.

[15] "Dielectric Properties", IT'IS Foundation. https://itis.swiss/virtual-population/tissue-properties/database/dielectric-properties/.

[16] "Dielectric Properties of Body Tissues", Italian National Research Council – Institute for Applied Physics http://niremf.ifac.cnr.it/tissprop/.

[17] S. Gabriel, R. W. Lau, and C. Gabriel, "The dielectric properties of biological tissues: III. Parametric models for the dielectric spectrum of tissues," *Physics in Medicine and Biology*, vol. 41, no. 11, pp. 2271–2293, Aug. 1996, https://doi.org/10.1088/0031-9155/41/11/003.

[18] Y. Q. Tan, S. A. Rezaeieh, A. Abbosh, and S. Mustafa, "Defining optimum frequency range for heart failure detection system considering thickness variations in human body tissues," in *2013 International Conference on Electromagnetics in Advanced Applications (ICEAA)*, Turin, Italy, Sep. 2013, pp. 1280–1282, https://doi.org/10.1109/ICEAA.2013.6632454.

[19] A. Y. I. Ashyap *et al.*, "Robust and Efficient Integrated Antenna With EBG-DGS Enabled Wide Bandwidth for Wearable Medical Device

Applications," *IEEE Access*, vol. 8, pp. 56346–56358, 2020, https://doi.org/10.1109/ACCESS.2020.2981867.

[20] Publications Office of the European Union, "CELEX1, 1999/519/EC: Council Recommendation of 12 July 1999 on the limitation of exposure of the general public to electromagnetic fields (0 Hz to 300 GHz)," Jul. 12, 1999. http://op.europa.eu/en/publication-detail/-/publication/9509b04f-1df0-4221-bfa2-c7af77975556/language-en (accessed Jul. 10, 2022).

[21] "IEEE Recommended Practice for Measurements and Computations of Radio Frequency Electromagnetic Fields With Respect to Human Exposure to Such Fields,100 kHz-300 GHz," *IEEE Std C95.3-2002 (Revision of IEEE Std C95.3-1991)*, 2002, https://doi.org/10.1109/IEEESTD.2002.94226.

[22] L. Belrhiti, F. Riouch, A. Tribak, J. Terhzaz, and Á. Mediavilla Sánchez, "Calculating the SAR distribution in two human head models exposed to printed antenna with coupling feed for GSM/UMTS/LTE/WLAN operation in the mobile phone," *International Journal of Microwave and Optical Technology*, vol. 11, no. 6, pp. 391–398, Nov. 2016.

[23] G. P. Gao, C. Yang, B. Hu, R. F. Zhang, and S. F. Wang, "A Wide-Bandwidth Wearable All-Textile PIFA With Dual Resonance Modes for 5 GHz WLAN Applications," *IEEE Transactions on Antennas and Propagation*, vol. 67, no. 6, pp. 4206–4211, Jun. 2019, https://doi.org/10.1109/TAP.2019.2905976.

[24] L. Wu, R. Li, Y. Qin, and Y. Cui, "Bandwidth-Enhanced Broadband Dual-Polarized Antennas for 2G/3G/4G and IMT Services," *IEEE Antennas and Wireless Propagation Letters*, vol. 17, no. 9, pp. 1702–1706, Sep. 2018, https://doi.org/10.1109/LAWP.2018.2864185.